

# Riding a wild horse: Majorana fermions interacting with solitons of fast bosonic fields.

A. M. Tsvelik

*Department of Condensed Matter Physics and Materials Science,  
Brookhaven National Laboratory, Upton, NY 11973-5000, USA*

I consider a class of one-dimensional models where Majorana fermions interact with bosonic fields. Contrary to a more familiar situation where bosonic degrees of freedom are phonons and as such form a slow subsystem, I consider fast bosons. Such situation exists when the bosonic modes appear as collective excitations of interacting electrons as, for instance, in superconductors or carbon nanotubes. It is shown that an entire new class of excitations emerge, namely bound states of solitons and Majorana fermions. The latter bound states are not topological and their existence and number depend on the interactions and the soliton's velocity. Intriguingly the number of bound states increases with the soliton's velocity.

## I. INTRODUCTION

Models describing Majorana fermions have received a lot of attention, mostly in the context of quantum computation. In the process of the discussion several models with interesting common features have emerged. In all these models Majorana fermions interact with solitons of bosonic fields representing collective degrees of freedom of electronic systems (usually phase fields of superconducting order parameters). Although models of interacting solitons and fermions have been considered before and there is an extensive literature on the subject, there are some new features which merit a discussion. The most important new feature shared by the models in question is that Majorana fermions are slow in comparison to the bosonic modes. This is opposite to a more familiar situation of the Peierls-Froelich model of polyacetylene where a slow optical phonons interact with fast fermions.

As I will demonstrate, in this situation new branches of fermion-soliton bound states emerge some of which exist only in a finite region of momentum space.

## II. MODELS

### A. p-wave Josephson junction

This model was formulated by Grosfeld and Stern [1] who considered a long insulating one-dimensional Josephson junction between two p-wave superconductors. As it is well known, p-wave superconductors have zero energy Majorana modes as boundary states. When the boundary is extended, as in the case of a long junction, these modes propagate along the edge with velocity  $v_\Delta \sim \Delta$ , the superconducting gap in the bulk. A conventional long Josephson junction is described by the sine-Gordon model; the p-wave one acquires an additional term in the Hamiltonian corresponding to Majorana fermions. The resulting model of the junction has the following

Lagrangian density:

$$\mathcal{L} = \frac{\tilde{c}}{2\beta^2} \left[ \tilde{c}^{-2} (\partial_\tau \Phi)^2 + (\partial_x \Phi)^2 + \frac{4}{\lambda_J^2} \sin^2(\Phi/2) \right] + \frac{i}{2} \left( r \partial_\tau r - v r \partial_x r + l \partial_\tau l + v l \partial_x l \right) + i m r l \cos(\Phi/2), \quad (1)$$

where  $r, l$  are right- and left-moving Majorana fermion fields propagating along different sides of the junction and  $\Phi$ -field represents the phase difference between the two superconductors. The parameters of the model are

$$\tilde{c} = c \sqrt{\frac{d}{d + 2\lambda_L}}, \quad \beta^2/8\pi = \frac{2e^2}{\hbar c} \sqrt{\frac{d(d + 2\lambda)}{h_z^2}}, \quad (2)$$

where  $d$  is the thickness of the barrier,  $\lambda_L$  is the London penetration depth,  $h_z$  is the height of the junction and  $\lambda_J$  and  $m$  are determined by characteristics of the junction. The magnetic field changes the argument of the sinus to

$$\Phi/2 \rightarrow \Phi/2 - e B d x / \hbar c. \quad (3)$$

Model (1) is a generalization of the Super sine-Gordon (SSG) model; for the latter case

$$m = v/\lambda_J, \quad \tilde{c} = v. \quad (4)$$

so that the model is Lorentz invariant. The SSG model is integrable [2] and its excitations and S-matrix are known [3]. In particular, it is known that solitons of SSG model obey non-Abelian statistics.

Since all candidates for p-wave superconductivity have small critical temperatures corresponding to small  $v$ , the ratio  $v/\tilde{c}$  is also likely to be very small (however, it may be increased somewhat by putting the junction on top of a dielectric with large  $\epsilon$ ).

### B. Combination of spin-orbit interaction and superconductivity

Although this model is not qualitatively different from the previous one, there are certain features which make

its material realization easier. Namely, the chiral Majorana modes emerge here not from a  $p$ -wave superconductor, which remains a rather exotic object, but by other means. Namely, Majorana fermions may emerge in a semiconductor with a strong spin-orbit interaction subject to external magnetic field brought into contact with an  $s$ -wave superconductor (see, for example [4],[5]). Following [4] I write down the Hamiltonian of two-dimensional film of such material:

$$H = \int \Psi^\dagger(x, y) \mathcal{H} \Psi(x, y) dx dy, \quad (5)$$

$$\Psi^\dagger = (\psi_\uparrow^\dagger, \psi_\downarrow^\dagger, \psi_\downarrow, -\psi_\uparrow),$$

$$\mathcal{H} = [\mathbf{p}^2/2m - \mu]\tau_z + u(p_y\sigma^z - p_x\sigma^y)\tau_z +$$

$$B(y)\sigma^x + \Delta(y)\tau_x,$$

where  $\tau_a$  act in particle-hole and  $\sigma^a$  in spin space respectively. As was shown in [4], when function  $V(y) = B(y) + \Delta(y)$  changes sign Majorana zero modes emerge. The corresponding operators of right- and left moving modes are made of combinations

$$r = \frac{1}{2}(\psi_\uparrow - i\psi_\downarrow + \psi_\uparrow^\dagger + i\psi_\downarrow^\dagger), \quad (6)$$

$$l = \frac{1}{2}(\psi_\uparrow + i\psi_\downarrow + \psi_\uparrow^\dagger - i\psi_\downarrow^\dagger), \quad (7)$$

These modes are spatially separated: the mode  $r$  emerges at the edge with  $dV/dy > 0$  and  $l$ -mode at the edge  $dV/dy < 0$ . These edges are boundaries between the topological insulator and the superconducting state. Being projected onto these modes the Hamiltonian density becomes

$$H_0 = \frac{u}{2} \int dx (-r\partial_x r + l\partial_x l). \quad (8)$$

Since the spin-orbit interaction is typically much greater in magnitude than the  $p$ -wave order parameter, one can increase the ratio  $u/\tilde{c}$ . In [4] the authors cite  $u = 7.6 \times 10^6 \text{ cm/sec}$  for InAr. With  $\lambda_L \sim 10^4 \text{ \AA}$  and  $d \sim 10 \text{ \AA}$  one can get  $u/\tilde{c} \sim 10^{-2}$ .

Now following [6] consider a situation when a narrow superconducting region is sandwiched between two topological insulators. Then instead of one bosonic mode as in (1) we will have more. Namely, if the superconducting region between two topological insulators is sufficiently narrow, we have the following action [6]:

$$-J \cos(\phi_a - \phi_b) + \text{irl} \left[ t_1 \cos\left(\frac{\phi_a - \phi_b}{2}\right) + t_2 \cos\left(\frac{\phi_a + \phi_b}{2} - \phi_m\right) \right] \quad (9)$$

where  $\phi_{a,b}$  are superconducting phases on the left and right from the superconducting strip and  $\phi_m$  is a phase on the strip. Therefore there are two independent bosonic modes.

### C. Half filled carbon nanotube

In [7] the author and Nersesyan derived an effective field theory for armchair carbon nanotubes using the bosonization approach with a partial re-fermionization. At half filling the model is similar to (1), but the number of Majorana fermions is not one, but 6 with different mass parameters  $m_a$  such that

$$m_{-2} = m_{-1} = m_c, \quad m_1 = m_2 = m_3 = m_t, \\ 2m_c + m_t + m_0 = 0. \quad (10)$$

The role of the bosonic field  $\Phi$  is played by the total charge field  $\Phi_c$ . The smallness of parameter  $\beta$  and a large value of  $\tilde{c}/v$  originate from the unscreened Coulomb interaction. The Lagrangian density is

$$\mathcal{L} = \frac{1}{2v}(\partial_t \Phi_c)^2 - \frac{v}{2K^2}(\partial_x \Phi_c)^2 + \frac{i}{2} \sum_{a=-2}^3 \bar{\chi}_a (\gamma_0 \partial_t + v\gamma_1 \partial_x) \chi_a - \mathcal{V}, \quad (11)$$

$$\mathcal{V} = i \cos[\sqrt{4\pi}\Phi_c] \left[ m_1 \sum_{a=-2}^{-1} \bar{\chi}_a \chi_a + m_2 \sum_{a=1}^3 \bar{\chi}_a \chi_a + m_3 \bar{\chi}_0 \chi_0 \right], \quad (12)$$

where  $\gamma_0, \gamma_1$  are Dirac gamma matrices,  $K \ll 1$  is the Luttinger parameter determined by the long range Coulomb interaction,  $\Phi_c$  is the total charge field and  $\chi_a$  are Majorana fermions made of chiral components of  $\Phi_f$  ( $a = -2, -1$ ) and  $\Phi_s, \Phi_{sf}$  fields ( $a = 0, 1, 2, 3$ ) [7]. The  $\mathcal{V}$ -term represents the leading interaction generated by the Umklapp processes; the interactions between the Majorana fermions are small in comparison. The symmetry of (11) is  $U(1) \times U(1) \times SU(2) \times Z_2$ . The Majorana modes with  $a = 1, 2, 3$  realize the  $S=1$  representation of the  $SU(2)$  group.

For  $K \ll 1$   $\Phi_c$  is essentially a classical field and its dynamics is determined by the equation

$$-v^{-1} \partial_t^2 \Phi_c(t, x) + vK^{-2} \partial_x^2 \Phi_c(t, x) + \sqrt{4\pi} \sin[\sqrt{4\pi}\Phi_c(t, x)] \sum_a m_a \langle \chi_a(t, x) \bar{\chi}_a(t, x) \rangle = 0, \quad (13)$$

At  $K \ll 1$  one can neglect coordinate dependence of the mass term and treat it as a constant for the purposes of calculation of the fermion average in (13). The result is

$$-v^{-2} \partial_t^2 \Phi(t, x) + K^{-2} \partial_x^2 \Phi(t, x) + M^2 \sin[\Phi(t, x)] = 0, \\ M^2 \approx \sum_a \frac{m_a^2}{v^2} \ln(\Lambda/|m_a|), \quad (14)$$

where  $\Phi = \sqrt{16\pi}\Phi_c$  and  $M^2$  is calculated with the logarithmic accuracy. This description is valid for excitations moving with velocities  $< v$ . So we see that the solitons of  $\Phi_c$  are solutions of the sine-Gordon equation. As far

as the fermionic excitations are concerned, they are determined by the same equations as for model (1). In the notations of (1) we have

$$1/\lambda_J = KM. \quad (15)$$

As is shown the subsequent Section, the fermions have bound states with the solitons such that the number of finite energy bound states in each channel is

$$N_{0,a} = m_a \lambda_J / v = \frac{m_a}{K \left[ \sum_b m_b^2 \ln(\Lambda/|m_b|) \right]^{1/2}}. \quad (16)$$

It is clear that for the Lorentz invariant case  $K = 1$  there are no finite energy bound states. More than that, they appear only if the Coulomb interaction is quite strong.

### III. SEMICLASSICAL ANALYSIS

In all models described above the bosonic action is of the sine-Gordon type. The sine-Gordon subsystem has two types of excitations: kinks and breathers. Kinks strongly interact with the Majorana fermions since the latter ones create bound states with kinks. There are two types of bound states: one type is the Majorana zero modes which modify the kink's quantum numbers and the other are massive ones. Below I do the analysis for model (1), generalizations for models (9,11) are straightforward. In particular, in model (11)  $\tilde{c} = v/K$ .

It is convenient to introduce new fermionic fields:

$$\chi_1 = (r + l)/\sqrt{2}, \quad \chi_2 = (r - l)/\sqrt{2} \quad (17)$$

I consider a static kink configuration first. Then for a kink centered around  $x_0$  the fermion operators can be represented by the mode expansion (19)[8]. The eigenfunctions satisfy

$$\begin{aligned} E\psi_1 &= i(v\partial_x - W)\psi_2, \quad E\psi_2 = i(v\partial_x + W)\psi_1, \\ E^2\psi_1 &= (-v^2\partial_x^2 + W^2 - v\partial_x W)\psi_1 \end{aligned} \quad (18)$$

where  $W = m \cos(\Phi/2)$ .

$$\begin{aligned} \begin{pmatrix} \chi_1(x, t) \\ \chi_2(x, t) \end{pmatrix} &= \gamma_0 \begin{pmatrix} \psi_0(x - x_0) \\ 0 \end{pmatrix} + \\ &\sum_{E_n > 0} \left\{ \left[ e^{-iE_n t} \hat{\gamma}_n(x_0) + e^{iE_n t} \hat{\gamma}_n^+(x_0) \right] \begin{pmatrix} \psi_{1,n}(x - x_0) \\ 0 \end{pmatrix} + \right. \\ &\frac{i}{E_n} \left[ e^{-iE_n t} \hat{\gamma}_n(x_0) - e^{iE_n t} \hat{\gamma}_n^+(x_0) \right] \times \\ &\left. \begin{pmatrix} 0 \\ (v\partial_x + W)\psi_{1,n}(x - x_0) \end{pmatrix} \right\} \end{aligned} \quad (19)$$

A general single-soliton solution is

$$\Phi = 4 \tan^{-1} \left[ \exp \left( \frac{x - x_0 - ut}{\lambda_J \sqrt{1 - (u/\tilde{c})^2}} \right) \right]. \quad (20)$$

In the static case  $u = 0$  this gives rise to the following potential:

$$W = m \tanh(x/\lambda_J). \quad (21)$$

Substituting it in (18) and using the results from [9], I obtain the following eigenvalues for the bound states:

$$\begin{aligned} E_n^2 &= \left( \frac{2m}{N_0} \right)^2 n(2N_0 - n), \\ n &= 0, 1, \dots < N_0 = m\lambda_J/v. \end{aligned} \quad (22)$$

and the eigenfunctions are

$$\begin{aligned} \psi_1 &= (\cosh \xi)^{(-N_0+n)} \times \\ F \left( -n, 2N_0 - n + 1, N_0 - n + 1; \frac{1}{e^{2\xi} + 1} \right), \\ \xi &= x/\lambda_J. \end{aligned} \quad (23)$$

Notice that in the Lorentz invariant case (4)  $N_0 = 1$  and the only bound state is the topological one  $n = 0$ .

Now let us consider the case of moving soliton  $u \neq 0$ . Let us introduce new coordinates:

$$\begin{aligned} x' &= \gamma(x - ut), \quad t' = \gamma(t - xu/v^2), \\ \gamma &= [1 - (u/v)^2]^{-1/2}. \end{aligned} \quad (24)$$

This Lorentz transformation leaves the fermionic action invariant and puts us in the reference frame of the moving soliton. The mass term in (18) becomes

$$W \left( \frac{x'}{\lambda'} \right), \quad \lambda' = \lambda_J \left[ \frac{1 - (u/\tilde{c})^2}{1 - (u/v)^2} \right]^{1/2}. \quad (25)$$

Notice that in the Lorentz invariant case  $\tilde{c} = v$  the scale does not change. However, if  $v < \tilde{c}$ , the soliton size increases and, as a consequence, the number of bound states  $N$  also increases:

$$N = N_0 \left[ \frac{1 - (u/\tilde{c})^2}{1 - (u/v)^2} \right]^{1/2}. \quad (26)$$

This is a somewhat unexpected result. The energy in this reference frame is given by (22) with  $N_0$  replaced by  $N$ .

In the laboratory reference frame the energy and momentum of the fermionic part of the bound state are (I set  $\tilde{c} \rightarrow \infty$ ):

$$\begin{aligned} E_n(u) &= \frac{2m}{N_0} \sqrt{n \left[ \frac{2N_0}{\sqrt{1 - (u/v)^2}} - n \right]}, \\ P_n(u) &= u E_n(u)/v^2, \quad n = 0, \dots, N_0/\sqrt{1 - (u/v)^2} - 1, \end{aligned} \quad (27)$$

To obtain the total energy and momentum of the kink and the bound state one has to add the energy and momentum of the kink:

$$E_k(u) = \frac{M_k}{\sqrt{1 - (u/\tilde{c})^2}}, \quad P_k(u) = \frac{M_k u}{\tilde{c}^2 \sqrt{1 - (u/\tilde{c})^2}}. \quad (28)$$

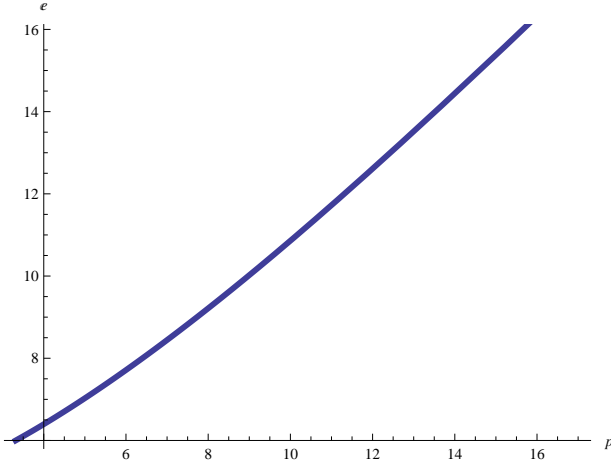


FIG. 1: The spectrum  $e = N_0[E(p) - M_k]/2m$  (27) for  $N_0 = 5$  and  $n = 6$ . The spectrum exists only for momenta larger than critical as explained in the text. The fermion velocity is set  $v = 1$ .

Consider  $n = 0$  mode first. For zero velocity this mode always exists, but for finite velocities its existence is restricted by the condition  $u < v$ . Assuming that  $\tilde{c}/v$  is so large that the kink's momentum is much smaller than the fermionic part and its dispersion is slow, we can set  $E_k = M_k, P_k = 0$ . Then from (28) we extract its dispersion:

$$E(p) = \sqrt{M_k^2 + (\tilde{c}p)^2}, \quad (29)$$

$$|p| < \frac{M_k}{\tilde{c}} [(\tilde{c}/v)^2 - 1]^{-1/2} \approx vM_k/\tilde{c}^2.$$

Thus the zero energy bound state always exists, though in a limited region of the Brillouin zone.

Now consider the finite energy bound states. They are not topological and their existence is conditional. Somewhat unexpectedly (27) shows that the conditions for their existence improve when the kink's velocity increases towards  $v$ . There are solutions with  $N_0[1 - (u/v)^2]^{-1/2} > n > N_0$  existing only for finite velocities (momenta). It is illustrated on Fig. 1.

To derive the dispersion of the bound states we have to take into account the fact that their energies and momenta are sums of (27) and (28). If we assume that

$$2m/N_0 \gg M_k(v/\tilde{c})^2, \quad (30)$$

then the inertia of the kinks is very small and their contribution to the total momentum can be neglected in comparison with the momentum of the bound state (27). As a result one gets the picture of the dispersion depicted on Fig. 2.

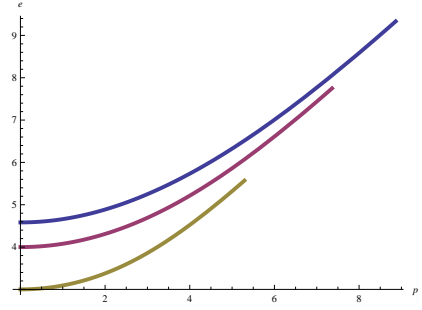


FIG. 2: The spectrum  $e = N_0[E_n(p) - M_k]/2m$  (27) for  $N_0 = 5$  and  $n = 1, 2, 3$ . The fermion velocity is set  $v = 1$ .

#### IV. QUANTUM NUMBERS AND CORRELATION FUNCTIONS

As we see from (19) the operators of fermion-kink zero modes  $\gamma_0(x_0)$  compose a Clifford algebra. For models with several species of Majorana fermions, such as (11),  $\gamma_0^a$  create a spinor representation of the corresponding group (for (11) the group is  $O(6) \sim SU(4)$ ) and the bound states of solitons and Majorana fermions transform according to this spinor representation. For the case of half filled carbon nanotube these excitations carry the same quantum numbers as the original fermions and therefore are quasiparticles. The situation with  $n \neq 0$  bound states is quite different. They transform according to the vector representation of the corresponding group and therefore can be created only by pairs of fermionic operators.

In order to get a better grip of the picture, let us consider the model of carbon nanotube. The symmetry group of model (11) is  $U(1) \times U(1) \times O(3) \times Z_2$ . As an example of a local field having nonzero matrix elements between the vacuum and the aforementioned bound states we have

$$e^{i\sqrt{4\pi}\varphi_c} \cos[\sqrt{4\pi}\varphi_f] \sim R_{1\uparrow}^+ R_{1\downarrow}^+ + R_{2\uparrow}^+ R_{2\downarrow}^+, \quad (31)$$

where  $\varphi_{c,f}$  are right-moving components of the corresponding bosonic fields,  $c$  labels the total charge,  $f$  labels the relative one and 1, 2 label positions of two Dirac points in the Brillouin zone of carbon nanotube. The first exponent creates two right-moving solitons in the charge sector. One soliton creates a bound state with a Majorana fermion from  $f$ -sector (asymmetric charge) and the other soliton remains unbounded. From this example one can see that the bound states can be observed only as parts of continua. In the above example the continuum consists of a "naked" soliton and a soliton-fermion bound state. Existence of "naked" solitons, i.e. ones which do not carry any fermionic modes is guaranteed by the fact that  $\tilde{c} > v$  and so there is plenty of room in momentum space for solitons which velocity exceeds the one of the fermions and those, as we know, do not create bound states.

## V. CONCLUSIONS

This paper demonstrates that in field theories without Lorentz invariance (quite a common thing in condensed matter physics) one has to expect appearance of new types of bound states, some of them existing only in

a limited region of momentum space.

I am grateful to Alexander Nersesyan and Robert Konik for interesting discussions. AMT was supported by US DOE under contract number DE-AC02 -98 CH 10886.

- 
- [1] E. Grosfeld and A. Stern, Proc. Natl. Acad. Sci. USA, 2011 Jul 19; **108**(29); 11810-4.
  - [2] A. Tsvelik, Sov. J. Nucl. Phys. ( Yad. Fis. ) 47, 172 (1988).
  - [3] C. Ahn, Nucl. Phys. B**354**, 57 (1991).
  - [4] Y. Oreg, G. Refael and F. von Oppen, Phys. Rev. Lett. **105**, 177002 (2010).
  - [5] R. M. Lutchyn, T. D. Stanescu, and S. Das Sarma, Phys. Rev. Lett. **106**, 127001 (2011).
  - [6] L. Jiang, D. Pekker, J. Alicea, G. Refael, Y. Oreg, and F. von Oppen, arXiv: 1107.4102.
  - [7] A. A. Nersesyan and A. M. Tsvelik, Phys. Rev. B**68**, 235419 (2003).
  - [8] E. Witten, Nucl. Phys. B**142**, 285 (1978).
  - [9] L. D. Landau and E. M. Lifshitz, "Quantum Mechanics (Non-relativistic theory)", Pergamon Press, 1977, pp. 73,74.